Effect of Protein Charge on the Generation of Aggregation-Prone Conformers

Kerensa Broersen,[†,‡,||] Mireille Weijers,[†] Jolan de Groot,[†,‡] Rob. J. Hamer,[†] and Harmen H.J. de Jongh*[,†,§]

Wageningen Centre for Food Sciences, Diedenweg 20, P.O. Box 557, 6700 AN Wageningen, The Netherlands, Laboratory for Food Chemistry, Wageningen University and Research Centre, Bomenweg 2, 6700 EV Wageningen, The Netherlands, and TNO Quality for Life, Utrechtseweg 48, 3704 HE Zeist, The Netherlands

Received December 27, 2006; Revised Manuscript Received March 19, 2007

This study describes how charge modification affects aggregation of ovalbumin, thereby distinguishing the role of conformational and electrostatic stability in the process. Ovalbumin variants were engineered using chemical methylation or succinylation to obtain a range of protein net charge from −1 to −26. Charge modification significantly affected the denaturation temperature. From urea-induced equilibrium denaturation studies, it followed that unfolding proceeded via an intermediate state. However, the heat-induced denaturation process could still be described as a two-state irreversible unfolding transition, suggesting that the occurrence of an intermediate has no influence on the kinetics of unfolding. By monitoring the aggregation kinetics, the net charge was found not to be discriminative in the process. It is concluded that the dominant factor determining ovalbumin aggregation propensity is the rate of denaturation and not electrostatic repulsive forces.

Introduction

The process of protein aggregation has been increasingly associated with several aggregation-related diseases.[1,2] Within this perspective, it is important to improve the current understanding of fundamentals of protein aggregation. Factors determining the aggregation process have been investigated in detail during the past decade.[3−8] Aggregation requires first (partial) unfolding of the polypeptide[9−12] and, second, the ability of these molecules to approach each other close enough to enable efficient intermolecular interaction. The electrostatic contribution has been noted as an important determinant in the process.[12−15] It was shown in these studies that upon varying charge interactions of (partly) unfolded molecules, for example, by changing the solvent conditions, the propensity of polypeptides to form aggregates can be controlled. Moreover, it was stated that electrostatic repulsion between particles can act as a prime determinant for the rate of aggregation.[16,17] The energy barrier generated by this electrostatic repulsion that hampers two proteins to reach each other's proximity to develop and stabilize van der Waals or chemical interactions is referred to as "colloidal stability". However, the role of the unfolding step was not evaluated. Affecting unfolding kinetics and thus the availability of aggregation-prone molecules by introducing or eliminating charged residues in a protein molecule could provide an alternative explanation for the observed effects of electrostatics on aggregation. Since it is difficult to separate the impact of protein charge on the conformational stability from that on the colloidal stability, a clear view on the mechanism has not emerged yet.

The required (partial) unfolding of the polypeptide chain is governed by the conformational stability of the molecule. A large difference in free energy between the folded and denatured state as well as a high kinetic barrier to unfolding will limit the generation of aggregation prone protein conformers. On the basis of comparisons of thermophilic and mesophilic protein families, it could be suggested that nature employs this approach of optimization of charge−charge interactions as evolutionary selection.[18] Work carried out by the group of Loladze et al. confirms that optimization of charge−charge interactions on the surface of proteins can be a useful strategy in the design of thermostable proteins with a high resistance to unfolding.[19] It thus appears that, next to interference of the colloidal repulsion between (partly) unfolded proteins, modulation of the ion pairing on the protein surface can be used to control the aggregation propensity.

Effective modulation of charge−charge intra- and intermolecular interactions between proteins can be achieved in two ways. First, by using site-directed mutagenesis, the newly engineered and translated primary structure is allowed to fold in an expression system. However, especially when multiple-point mutations are employed, this approach frequently results in alternative folding of the protein compared to the wild-type protein. Alternatively, chemical modification uses the folded conformation of the protein as a starting point and adds new properties. This approach of chemical modification has been followed by many researchers in the past[20,21] and can be employed efficiently when care is taken that structural differences caused by charge modification do not impair with the objected aim of the study.[22]

The model system used in this study is ovalbumin, a well-characterized serpin with a molecular size of 45 kDa that is known to form aggregates under various conditions.[23,24] Ovalbumin is widely used in industrial applications and the unfolding and aggregation behaviors are well documented.[25] In this work, both positive and negative charges of ovalbumin have been

* To whom correspondence should be addressed. Tel.: +31 317 486160. Fax: +31 317485384. E-mail: harmen.dejongh@tifn.nl.
† Wageningen Centre for Food Sciences.
‡ Wageningen University and Research Centre.
§ TNO Quality for Life.
|| Current address: MRC- Laboratory of Molecular Biology, Neurobiology Division, Hills Road, Cambridge, CB2 2QH, United Kingdom.

10.1021/bm0612283 CCC: $37.00
Published on Web 04/28/2007

Table 1. Modification and Electrostatic Description of Selected Ovalbumin Variants

	# groups available/molecule			charge/moleculeat pH 7.0[d]	isoelectric point
ovalbumin variant	carboxyl[a] groups/molecule	lysine[b] groups/molecule	number of modified groups[c]	calculated	(IEF)
OVA-26	58 ± 2	15 ± 1	7 ± 1	−26 ± 2	3.7
OVA-12	50(48)[e] ± 2	21(21)[e] ± 1		−12	4.7
OVA-5	43 ± 2	22 ± 1	7 ± 2	−5 ± 2	5.0
OVA-1	39 ± 2	22 ± 1	11 ± 2	−1 ± 2	5−7

[a] Number of carboxyl groups determined using chromogenic Woodward K assay. [b] Number of lysine groups determined using chromogenic OPA assay. [c] Number of modified groups determined using the results of the Woodward K assay and OPA assay. The number indicates the number of succinyl (in case of succinylation) or methyl groups (in case of methylation) attached to the protein. [d] Charge is calculated on the basis of primary structure (1OVA) input in Swiss-Prot. [e] Between brackets: theoretical values of carboxyl groups and lysine groups derived from the primary structure of ovalbumin (PDB-code 1OVA).

modified using methylation of carboxylates and succinylation of lysines, and the impact of this on its structural integrity and its unfolding behavior is described. This provides us with the opportunity to discriminate the role of (net) charge on the generation of aggregate-prone proteins from that on the kinetics of aggregation.

Results

Preparation of Materials. To investigate the effect of charge on the functional properties of proteins related to the generation of molecules that can undergo aggregation reactions, a series of ovalbumin (OVA) variants was generated that differed in a wide range of net charge while preserving the native fold. The succinylation and methylation reactions of, respectively, lysine and carboxylate groups have been documented in detail before.[22] While each methylation of a carboxylate on glutamic or aspartic acid results in an elimination of a single charge, the impact of succinylation of a lysine residue is double as it renders it from a positively charged to a negatively charged group. Although chemical modification is a "random" process, those charged groups that are least involved in ion pairing on the protein surface are most susceptible to chemically react. As a result, the heterogeneity introduced appears to be limited when these materials are assayed using affinity chromatography.[26] A series of differently charged ovalbumins can thus be obtained by varying experimental parameters like incubation time, temperature, and reactant-to-protein ratio. The protein series used is denoted as OVA-26, OVA-12, OVA-5, and OVA-1 (Table 1) where the number indicates the calculated net charge of the polypeptide as determined from the degree of modification using ortho-phthaldialdehyde (OPA, for the number of lysines) and Woodward (for the number of carboxylates) analyses (Table 1). OVA-12 is the native protein, not subjected to any modification.

Since it is crucial for this study to retain under ambient conditions the intact globular structure after charge modification, the produced ovalbumin variants were tested for their tertiary and secondary structure using intrinsic tryptophan fluorescence (Figure 1a), near-UV circular dichroism (CD) (provided as Supporting Information), and far-UV CD (Figure 1b). As shown in Figure 1a, all selected OVA variants showed a λ_{max} around 340 nm, comparable to the wild-type ovalbumin (OVA-12). Interestingly, the quantum yield of the wild-type protein (OVA-12) was higher than the modified proteins. This difference in quantum yield has more frequently been observed by us for charge-engineered proteins, but an explanation of its origin has not been found thus far. Previously, it was shown by comparison of the fluorescence spectra of these charge variants upon excitation at 274 and 295 nm that the efficiency of energy transfer from tyrosine to tryptophan was not affected for these variants.[26] This suggested comparable structural constraints in the core of these proteins. These results were confirmed by the similarity in the near-UV CD-spectra of the four selected variants (presented as Supporting Information). In view of the readily comparable shape of the far-UV CD-spectra (Figure 1b), where all variants show a similar zero-crossing around 203 nm, it can be concluded that also at a secondary folding level the charge modification had no significant impact (with estimated secondary structure content of all variants of 35% β-strand, 35% α-helix, and 13% β-turn). From analysis of the quaternary structure (gel permeation chromatography, unpublished results), it was concluded that all these variants were monomeric under ambient conditions (10 mM phosphate, pH 7.0) eluting with an Rf-value of 0.62. Figure 2 illustrates that the apparent isoelectric point (IEP) changed in the expected direction from 3.7 for OVA-26 up to ~7 for OVA-1. This latter variant showed a broad band on the gel and maybe even multiple contributions that could be caused by the lower solubility of the material and that increased heterogeneity for this most charge-engineered variant. These results are in line with previously reported zeta-potential measurements of a comparable series charge variants.[26] The results of the molecular characterization are summarized in Table 1. It can be concluded that the four charge variants selected here bear the same structural properties under ambient

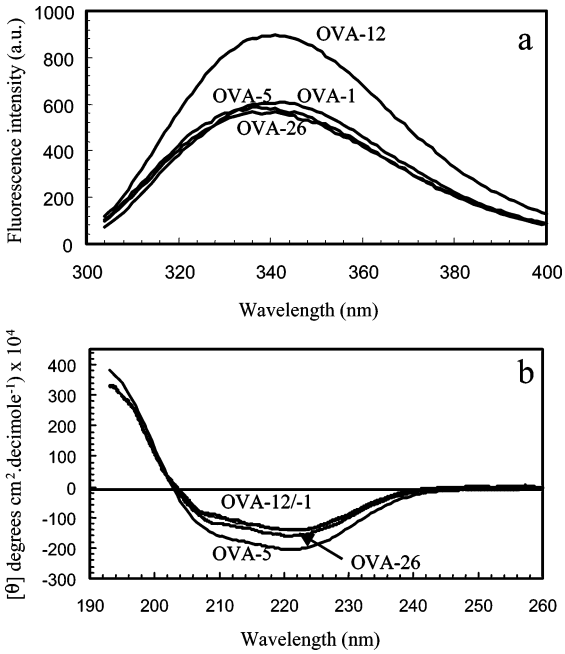

Figure 1. Structural characterization of ovalbumin charge variants. Intrinsic tryptophan fluorescence spectra (excitation at 295 nm) (a) and far-UV circular dichroism spectra (b) of charge variants of ovalbumin. The protein concentrations are 2.7 μM for tryptophan fluorescence and 2.3 μM for far-UV CD in 10 mM potassium phosphate (pH 7.0), and the data are recorded at 25 °C. The corresponding curves for OVA-26, OVA-12, OVA-5, and OVA-1 are indicated in the figure.

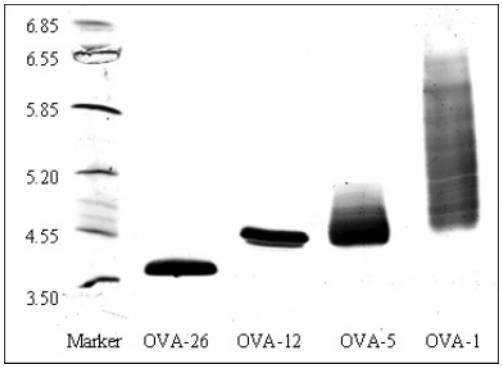

Figure 2. Isoelectric focusing of charge variants of ovalbumin. The 0.3 mM samples of the various ovalbumin charge variants (as indicated) were applied to a ready-to-use PhastGel IEF (4.5−6.5), stained with Coomassie Brilliant Blue. The left lane indicates the position of a commercial calibration kit containing proteins with isoelectric points varying from 6.5 to 2.5.

conditions. More extreme modification leading to net positively charged proteins or even more negative ones resulted in variants that started to deviate from the wild-type protein in terms of its structure (results provided as Supporting Information), placing restraints on the charge range that could be evaluated in this study.

Physicochemical Properties of Selected Ovalbumin Variants. Intermolecular interactions are, apart from electrostatics, dictated by the exposed hydrophobicity of the protein and the presence of reactive cysteines. To isolate the effect of charge on the aggregation propensity, it is important that hydrophobicity as well as the presence of reactive cysteines is not affected by charge modification. Since the binding affinity of the more commonly used probe ANS is sensitive to the protein net charge, we used in this study PRODAN, an uncharged probe that becomes an efficient fluorophore upon binding to hydrophobic areas on the protein surface,[27] to evaluate the impact of the charge modification on the hydrophobic exposure of the ovalbumin variants (Table 2). As can be seen from the table, the surface hydrophobicity (S_0) determined in this way was not very different for the ovalbumin variants. All variants had an S_0 between 59 and 68. To illustrate the (in)significance of these differences, the S_0 value of another folded well-soluble globular protein, β-lactoglobulin, was reported to be 375,[27] as could be confirmed by us as well.

To enable covalent aggregation through disulfide interactions, in the first place reactive thiol groups from cysteine residues have to be present in the primary structure of the protein. Using Ellman's assay under both protein denaturing and nondenaturing conditions, it was found that the number of thiol groups available in the proteins was not affected by charge modification (Table 2). Native ovalbumin contains six cysteine residues in the primary structure of which two are involved in an internal disulfide bridge. The sulfhydryl groups are not readily solvent-accessible in the variants under native conditions, but all expected groups can be detected in the unfolded conformers as was confirmed when determining the number of sulfhydryl groups in the presence of 10% sodium dodecyl sulfate (SDS). Next to their presence, their reactivity is another functional property that requires evaluation. The reactivity of thiol groups can be determined (at any relevant condition) using the sulfhydryl-disulfide exchange index (SEI).[22,28] It was found that the reactivity of the thiol groups at 25 °C was not affected by the charge modification (Table 2) within the standard error of 5% for this experiment. Also at elevated temperature (58 °C), but still below denaturation temperatures, no large differences in reactivity could be detected, except for OVA-1 which showed a slightly higher reactivity (SEI = 2.81) compared to the other ovalbumin variants (SEI = 3.14−3.28, Table 2). As such, it can be concluded that the introduction or inversion of charge within specific restraints does not necessarily result in differences in the ability to form disulfide bonds or affect the exposed hydrophobicity of the folded molecules.

Effect of Charge on Denaturant-Induced Unfolding. Figure 3 shows profiles of the normalized fluorescence intensity change versus denaturant concentration from 0 to 8 M urea for the equilibrium urea-induced unfolding of the ovalbumin variants. That equilibrium has been reached in these samples was demonstrated by the fact that in time no differences in fluorescence were observed (results not shown). Moreover, when these samples in urea were analyzed upon prolonged storage (up to 2 days), no irreversible aggregation could be detected when these samples were analyzed using native gel electrophoresis (unpublished results). In Figure 3, at least two transitions can be distinguished upon addition of increasing concentrations of urea. For the highly charged OVA-26, a first small transition takes place with a midpoint around 3.5 M urea that is succeeded by another transition with a midpoint of 4.2 M urea. This latter transition is shifted to a higher denaturant concentration of ~5.5 M urea for the variants with a lower net charge. The appearance of the intermediate is independent of the incubation time in urea buffer (unpublished results). Although all variants exhibit this thermodynamically stable intermediate, it is most explicitly observed for OVA-1. This intermediate has been further studied by monitoring the λ_{max} as a function of the urea concentration. It was found that for OVA-26, OVA-12, and OVA-5, the fluorescence intensity at 330 nm and the change in peak position (λ_{max}) as a function of urea concentration coincide, as exampled in Figure 4a for OVA-5. For the OVA-1 variant (Figure 4b), a transition midpoint at a urea concentration of 5.2 M was obtained by monitoring the fluorescence intensity at 330 nm compared to a midpoint of 6.2 M when plotting the peak position as a function of urea concentration. These results confirm that the presence of an intermediate unfolding state in OVA-1 appears more pronounced compared to the OVA variants with a higher negative net charge.

Effect of Electrostatics on Kinetic Partitioning upon Refolding. The formation of a thermodynamically stable intermediate could give rise to a difference in kinetic partitioning between aggregation and refolding. The contribution of the above-described unfolding intermediate to the refolding process has therefore been examined by means of urea- and heat-induced unfolding studies. Far-UV CD analysis shows that heat-induced unfolding at a protein concentration of 2.3 μM is an irreversible process for all variants tested (shown in Figure 5a for OVA-1 and Figure 5b for OVA-5). The CD spectra of the proteins at 90 °C (recorded after 10 min incubation at this temperature) and that after subsequent cooling of these samples to 20 °C appear very similar and show a shift of the zero-crossing from 203 to 201 nm. This indicates that there is no structural change noticeable during the cooling trajectory, suggesting that all denatured proteins are already in an aggregated state at 90 °C. This shift of the zero-crossing to lower wavelength reflects the loss of part of the β-stranded structures in the protein. Native gel electrophoresis confirmed that, upon refolding from a heat-induced unfolded state, all protein molecules in each variant proceeded into an intermolecular associated state (results not shown), indicating that the kinetic partitioning is driven toward aggregation. This observation is in agreement with a previous

Table 2. Number of Thiol Groups, Surface Hydrophobicity (S_0), and Sulfhydryl-disulfide Exchange Index (SEI) for Ovalbumin Variants

	number of thiol groups		S_0[c]	SEI[e]	
ovalbumin variant	nondenaturing[a]	denaturing[b]	initial slope	$SEI_{25\ °C}$	$SEI_{58\ °C}$[d]
OVA-26	0	5 ± 1	66	3.14	3.28
OVA-12	0	4 ± 1	68	3.43	3.21
OVA-5	0	4 ± 1	65	3.35	3.14
OVA-1	0	5 ± 1	59	3.15	2.81

[a] Number of SH groups detected using Ellman assay. [b] Number of SH groups detected using Ellman assay in the presence of 10% SDS. [c] Initial slope (S_0), PRODAN fluorescence intensity/% protein, was calculated from fluorescence intensity versus protein concentration plot. [d] OVA-26 and OVA-5 variants were heated at 54 °C and 56 °C, respectively, to avoid denaturation. [e] The reproducibility of the sulfhydryl exchange index (SEI) is typically about 5%.

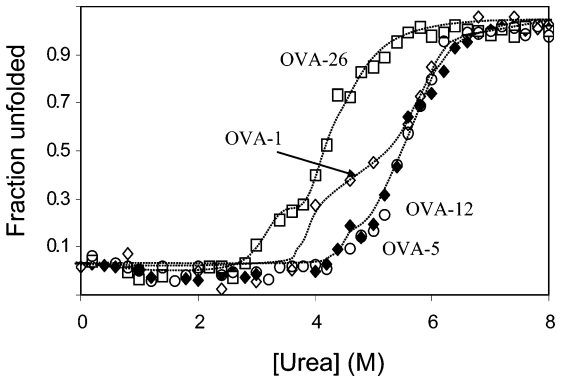

Figure 3. Urea-induced unfolding equilibrium of ovalbumin variants. The final protein concentration is 1.17 μM in 10 mM potassium phosphate (pH 7.0) and the data are recorded at 25 °C. The fluorescence emission intensity data recorded at 330 nm are normalized and expressed as normalized fluorescence intensity change versus urea concentration. OVA-26 (□), OVA-12 (○), OVA-5 (◆), OVA-1 (◇). The excitation wavelength was 295 nm.

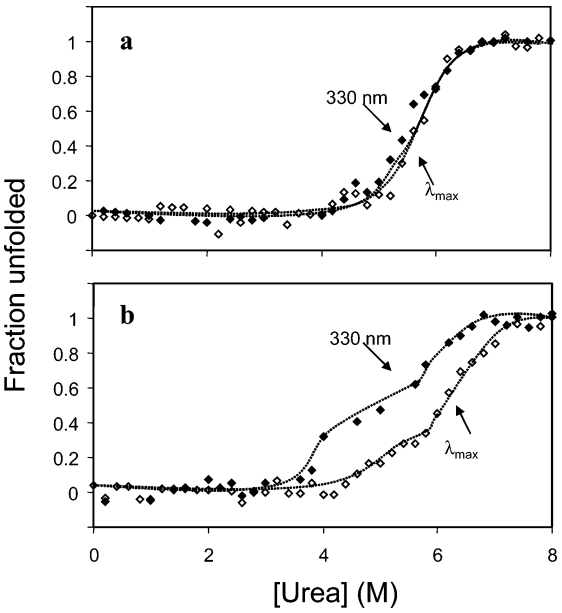

Figure 4. Urea-induced unfolding equilibrium of ovalbumin variants and intermediates. Urea-induced unfolding of (a) OVA-5 and (b) OVA-1 in 10 mM potassium phosphate at pH 7.0 and 25 °C. Data are obtained by monitoring the fluorescence intensity at 330 nm (◆) and the frequency shift of the fluorescence maximum (◇) in the presence of 1.17 μM of ovalbumin. The fluorescence intensity data are normalized and expressed as normalized fluorescence intensity change versus urea concentration.

report showing that unfolding of native ovalbumin was irreversible.[25] As also for OVA-1, all unfolded proteins adopt an aggregated state by both heat-induced and urea-induced unfolding, and it can be assumed that accumulation of an intermediate state does not affect the refolding route. To verify this, the

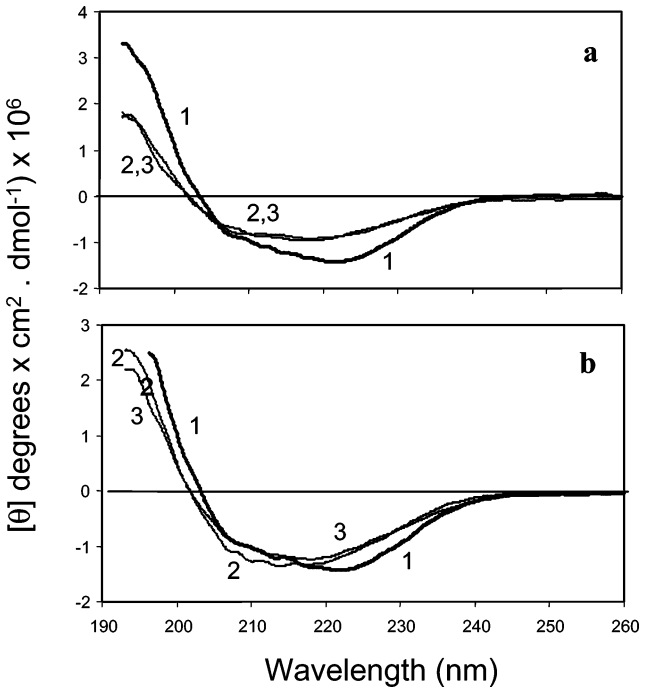

Figure 5. Heat-induced unfolding and refolding of ovalbumin charge variants showing irreversibility of the refolding process. Folded, unfolded, and refolded OVA-1 (a) and OVA-5 (b). The spectra were obtained at 20 °C (folded, spectrum 1), 90 °C (unfolded, spectrum 2), and 20 °C after cooling (refolded, spectrum 3). The protein concentration is 2.3 μM in 10 mM potassium phosphate at pH 7.0.

OVA-1 intermediate was populated at 4 M urea (Figure 4). Upon dilution of this sample into buffer, thereby lowering the denaturant concentration 10 fold, it was demonstrated by native gel electrophoresis (Figure 6) that also from the intermediate state the preferable route for the proteins is leading to an aggregated state. Exposing the proteins to a 9 M urea denaturing condition and subsequent refolding by dilution of the sample yielded in all cases 100% aggregated material as evidenced by native gel (results not shown).

Effect of Charge on the Heat-Induced Denaturation. Figure 7A shows the differential scanning calorimetry (DSC) thermograms of the OVA variants. OVA-26 shows a transition peak between 65 and 80 °C and has a peak temperature (T_p) of 73.8 °C. A decrease in net charge to −12 shifts the T_p upward to 78.8 °C. Upon decreasing the net charge down to −5, the peak temperature decreases again to 78.2 °C and the peak becomes broader. For OVA-1, the peak temperature decreases even further to 76.2 °C. These data are summarized in Table 3. In the cooling and subsequent second heating run (illustrated for OVA-12 in Figure 7B), in none of the samples endothermic transitions could be observed, indicating the irreversibility of the process for all OVA variants studied. Since the denatured molecules tend to aggregate (likely to result in exothermic contributions to the heat flow), the enthalpy change related to

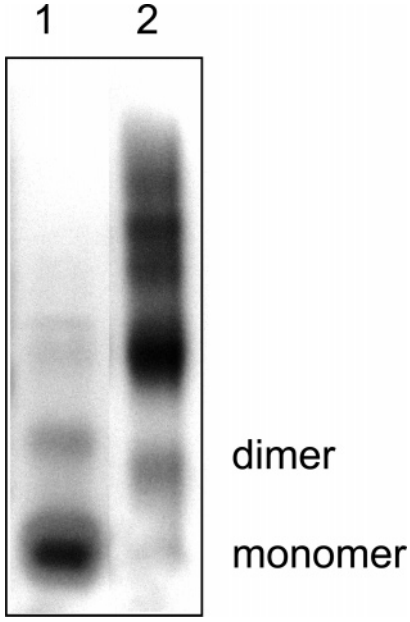

Figure 6. Irreversible refolding of the urea-induced accumulation of unfolding intermediate OVA-1. Native-PAGE electrophoresis of OVA-1 incubated in 4 M urea (lane 1) and upon 10-fold dilution with 10 mM potassium phosphate buffer at pH 7.0 and 20 °C in the absence of urea (lane 2).

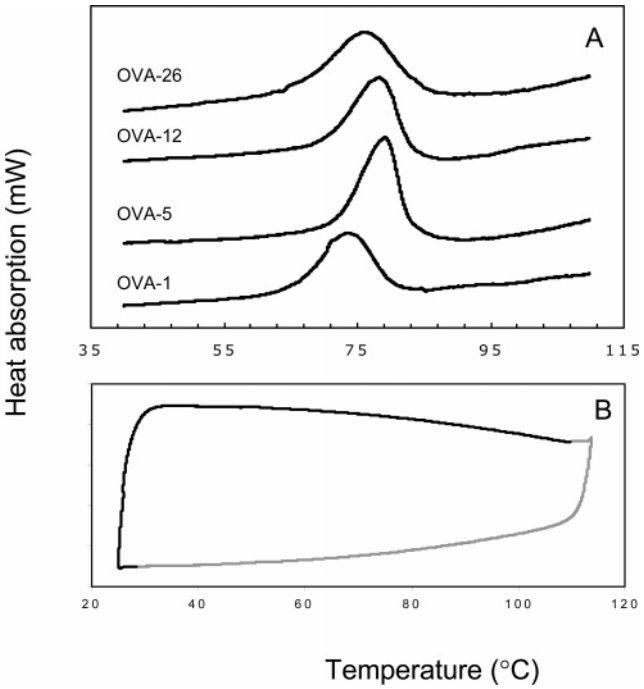

Figure 7. Heat-induced unfolding of ovalbumin variants. (A) Differential scanning calorimetry was performed at a protein concentration of 0.23 mM for the OVA variants in 10 mM potassium phosphate (pH 7.0). The heating rate was 1 °C/min. (B) Cooling (gray line) and second heating (black line) thermogram (at 1 °C/min) of the OVA-12 variant performed subsequently to the heating curve shown in panel A.

denaturation is hard to establish from these thermograms, making an analysis using the Eyring equation more complex. The results of calculating the apparent activation energies of the rate-limiting step as deduced by fitting the DSC profiles (Figure 7A) by an equation using first-order irreversible unfolding models[29] are tabulated in Table 3. OVA-26 has an activation energy of 296 kJ mol^{-1}. Decreasing the net negative charge leads to an increase of the activation energy by 14% for OVA-12. A further decrease in net negative charge results in a decreased activation energy of 1 (OVA-5) and 30% (OVA-1) compared to that of OVA-26. The unfolding process is an irreversible transition and the final "unfolded" state cannot be defined. Therefore, it is only plausible to ascribe the found activation energies to the transition with the highest activation energy, which is then regarded as the rate-limiting step in the process. Also, to interpret these activation energies in terms of thermodynamic stability parameters, one would need to include the activation entropy term as well. The current studies do not provide detailed insight in this parameter. Nevertheless, from Table 3 it is clear that the thermodynamics of the denaturation transition is significantly altered by charge modification. It was reported before that the denaturation of wild-type ovalbumin can be described by a two-state irreversible first-order model,[25] and this model is shown to fit the thermal denaturation curves of all variants adequately (Figure 7). Only the fitting of the thermogram of OVA-1 was less accurate. This may be due to the more pronounced population of an intermediate, also observed for urea-induced unfolding, affecting the unfolding kinetics (Figures 3 and 4b). Apparently, the population of intermediates observed for urea-induced unfolding for the other variants (OVA-26, OVA-12, and OVA-5) has no consequence for the fitting of the DSC data with an irreversible first-order model, suggesting that its occurrence has no influence on the kinetics of the process.

Effect of Charge on Aggregation Kinetics. To discriminate the impact of net charge on either the generation of reactive conformers or the kinetics by which these reactive particles irreversibly associate, protein solutions ranging from 5 to 40 mg/mL were heated at a temperature where the first process was expected to be similar for all variants. On the basis of the denaturation temperature and activation energies (Table 3) for each variant, the temperature was determined where, according to the Arrhenius equation, the process associated to the endothermic transition had a rate constant of 0.04 min^{-1}. This rate constant was arbitrarily chosen to allow us to monitor aggregation kinetics on a time scale that could be assayed well. These temperatures were typically about 7 °C below the reported T_p. By selecting this unique rate constant for all variants and taking into consideration the assumptions mentioned in the previous section related to the entropic contribution, we propose that differences in aggregation kinetics can in this way be attributed to differences in colloidal interactions in the aggregation process only. Figure 8 shows for these four variants how the fraction monomeric protein decreases in time upon incubation. Clearly, no significant differences between the four charge variants are observed. Moreover, no concentration dependence on the aggregation kinetics was detectable in this protein concentration range, indicating that the intermolecular association process was not rate-limiting for these variants. The monomeric fraction of the resulting incubated sample was separated using gel permeation chromatography, and the structural properties of this fraction were analyzed using far-UV CD and tryptophan fluorescence. The results obtained demonstrated that the monomeric fraction has similar structural properties as the native proteins (results not shown).

Discussion

Net Charge Modification Affects Protein Stability. Succinylation and methylation of ovalbumin have been used in this work to investigate the role of protein net charge on the unfolding and refolding behavior of proteins in the context of

Table 3. Thermodynamic Description of Selected Ovalbumin Variants

ovalbumin variant	T_p[a] (°C)	ΔH[a] (kJ mol^{-1})	E_{act}[b] (kJ mol^{-1})	k unfolding (min^{-1})[c]	midpoint (M urea) at 330 nm[d]
OVA-26	73.8	465	296	0.0402	4.2
OVA-12	78.8	514	338	0.0323	5.5
OVA-5	78.2	477	293	0.0345	5.5
OVA-1	76.2	560	208	0.0442	5.2

[a] The thermal transition temperature was described as the peak temperature in the DSC thermogram. The accuracy of the data is ±0.1 °C. The enthalpy change was determined by integration of the peak area of the thermogram. The reproducibility was typically ±40 kJ/mol. [b] The DSC curves are described using first-order irreversible unfolding models[29] resulting in the definition of an activation energy of unfolding. $\nu/T_t^2 = ARe^{-E/RT_t}/E$ where ν is the scan rate, E is the energy of activation, A is the frequency factor of the Arrhenius equation, R is the gas constant, and T_t is the thermal transition temperature. The reproducibility of the established numbers is less than 4%. [c] The k of unfolding was calculated by a theoretical description of the temperature dependence of the frequency factor and the activation energy. The typical experimental error was ±0.0011 min^{-1}. [d] Urea concentration at which 50% of the molecules reside in a folded state. The reproducibility of the midpoint is less than 0.1 M.

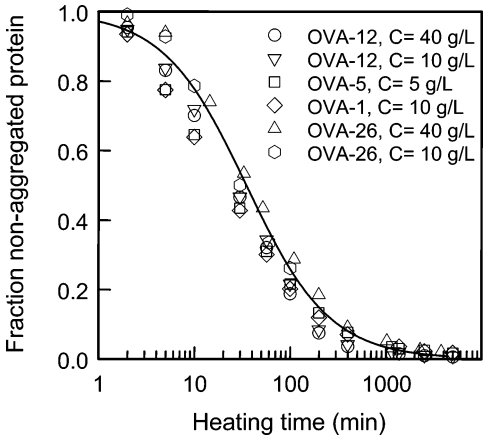

Figure 8. Heating time dependence of the fraction monomeric protein for charge-engineered OVA variants. The OVA solutions (protein concentrations ranging from 5 to 40 mg/mL, pH 7.0) were heated about 7 °C below their denaturation temperature (T_p) as tabulated in Table 3. The fraction monomeric material was obtained using UV280 absorption from the elution profile of size exclusion chromatography. The dashed line is to guide the eye.

the generation of aggregate-prone particles. Aggregate formation is generally constrained by the availability of a high concentration of (partly) unfolded molecules (conformational) and the absence of forces opposing aggregation (colloidal). Previous work mostly concentrated on one of these constraints in isolation. Intramolecular electrostatic factors can contribute significantly to the conformational stability.[10,30] Also, increased repulsion caused by introducing additional net charge decreases protein−protein interactions and thus changes the colloidal stability.[31,32] An approach that accounts for both conformational and colloidal stability would reveal the relative importance of these two contributions in the aggregation process.

To discriminate the role of protein net charge more explicitly, it is essential to also investigate to what extent other factors that might influence the aggregation propensity are affected by the charge engineering. It was shown that the four ovalbumin variants differing in net charge from −1 to −26 (Table 1) did not differ significantly in conformation as assayed at a secondary, tertiary, and quaternary level (Figure 1) nor in physicochemical properties as exposed hydrophobicity or chemical reactivity (Table 2). It was also shown that the unfolding pathway was in all cases via an intermediate (Figure 3) that appeared more pronounced for the OVA-1 variant compared to the others.

Charge modification was found to have significant consequences on the apparent stability of the variants (Table 3, Figures 3 and 7). No clear correlation was, however, found when relating the net charge to the stability of the variants determined by urea- (Figure 3) or heat-induced (Figure 7) unfolding. Basically, any charge modification on the wild-type protein (OVA-12) leads to a destabilization. Although those charges that are least involved in ion pairing on the protein surface are most eligible for modification, interference of the charge distribution is likely to result in a destabilization of the ionic network. This has been shown effectively by experiments where specific point mutations of various protein primary structures were related to stability parameters.[19,33,34] It was shown convincingly that the contribution of electrostatic forces to stability is related to the specific location of ion pairs and to the geometry of ion pair networks.

Rate of Unfolding Varied by Net Charge. An important condition to drive the aggregation process is the generation of a sufficient population of (partly) unfolded protein molecules. This rate of generation is determined by the activation energy of unfolding, leading to molecules that are prone to aggregation. It was found that both charge reversal (succinylation of lysines) and elimination (methylation of carboxylates) decrease the activation enthalpy compared to that of the wild-type protein (OVA-12) (Table 3). No relation is therefore found between net charge and the activation energy of denaturation. It has been reported before that the unfolding rate of rubredoxin from two different organisms can differ significantly, even though the proteins carried a similar net charge but exhibited a different ionic network on the protein surface.[35] It was suggested that the location of ion pairs as well as the geometry of the ion pair network is playing a larger role in determining the rate of unfolding than the total net charge. When breakup of ion pairs on the protein surface is regarded as the most important kinetic event in the process (because of the large solvation penalties of dehydration followed by a favorable rehydration of the separated charges), clearly any interference with the ionic network will lead to a lower activation energy of unfolding and thereby will speed-up the generation of denatured conformers.

Changing the Net Charge of Ovalbumin Does Not Affect the Unfolding/Refolding Pathway. Generally, the unfolding process of the OVA variants can be described using a first-order irreversible unfolding mechanism, except for OVA-1, where, more pronounced than for the other charge variants, a clear accumulation of a thermodynamic stable intermediate could be observed (Figures 4 and 5). It is possible that these intermediates can either direct the protein into a refolded state or into an aggregated state. However, as it was found that the unfolding of OVA-1 was irreversible, similar to the other OVA variants tested, we suggest that the intermediate does not play a role in the refolding of the protein. Even more, the accumulation of this intermediate state at moderate urea concentrations and subsequent dilution in urea-deficient buffer led to the formation of aggregates (Figure 6), suggesting that this intermediate resembles a state that is aggregation-prone. The ap-

pearance of a more thermodynamically stable intermediate for OVA-1 could be the result of weakened repulsive forces that would otherwise be responsible for the fast transition of partially into fully unfolded molecules; in the case of an almost net neutral protein, enhanced screening of these interactions could occur, enabling the population of a detectable intermediate. Although such characterization of intermediates falls outside the scope of this work, we would like to refer to the "phase diagram method" that could be very useful to identify such intermediates.[36]

Generation of Denatured Particles Is Dominant in the Aggregation Process. The application of heat puts a continuous drive on the protein system to generate (partly) unfolded reactive particles that are eligible to undergo aggregation reactions. It can be assumed that the denaturing condition as provided by heat provokes a similar denaturation pathway as by changing the solvent quality with the difference that in the latter case the (intermediate) unfolded species can be retained in that folding state. Despite differences in the aggregation kinetics of the four different charge variants at a given temperature, referencing the observed aggregation kinetics by evaluation under conditions that the generation of denatured species is comparable gives the remarkable result that net charge is not discriminative (Figure 8). Colloidal repulsive interaction apparently does not limit the aggregation kinetics. The flexibility of the denatured polymer chain overcomes persistent repulsive forces, and the extent of hydrophobic exposure is such that the drive to aggregate overrules other colloidal interactions. Also, the absence of a protein concentration dependence on the observed aggregation kinetics (Figure 8) demonstrates unambiguously that the generation of aggregate-prone particles is the rate-limiting step in the process. However, the type of aggregate formed for these four charge variants is quite different; where OVA-26 forms fibrillar aggregates, OVA-1 aggregates are random clusters of proteins. Description of the aggregate types formed by these charge variants and the impact for protein network formation is the subject of another paper.[37]

Summarizing, in this work, we have shown that the dominant factor determining aggregation propensity is the rate of denaturation and not colloidal repulsive forces. The generation of aggregate-prone particles can be primarily varied by changing charged groups on the protein surface. Involvement of these groups in the ionic network on the protein surface leads to a significant drop in activation energy related to the endothermic process of the denaturation step. The results implicate that, when considering charge effects on the aggregation properties of proteins, it is crucial to combine the results of conformational stability studies as well as colloidal stability studies to evaluate the mechanism controlling protein aggregation. Where the first study explores a protein-specific property, the latter one is more implicit to solvent quality. Especially for multidomain proteins where only partial unfolding might occur under denaturing conditions, the balance between exposed hydrophobicity and net charge needs to be considered. In the case where nonpolar residues in a denatured state could be accommodated by either residual structure or, for example, sugar moieties,[47] the role of net charge on the aggregation propensity might become more important.

Experimental Methods

Materials. Ovalbumin was purified from fresh hen eggs according to a previously described purification protocol.[22]

Carboxylic acid groups in ovalbumin were methylated using a previously described procedure.[38,39] A 1 L solution of 0.22 mM ovalbumin containing 1 M methylamine was set to pH 4.6 using 1 M HCl and was stirred at room temperature. Subsequently, to produce two charge variants with different degrees of methylation, either 150 or 300 mg solid *N*-(3-dimethylaminopropyl)-*N*-ethylcarbodiimide hydrochloride (EDC) was added stepwise in small portions, while the pH was kept at 4.6 (±0.1) by the addition of 1 M NaOH using a pH-stat (Metrohm). When all added EDC was dissolved, the solution was stirred for another 2 h. Next, the pH was raised to 8.0 by dropwise addition of NaOH (1 M). After another 1 h of stirring at room temperature, the mixture was dialyzed extensively against demineralized water at 4 °C followed by freeze-drying.

Primary amino groups in ovalbumin were succinylated essentially as described before.[22,40] Four hundred milliliters of solution of 55 mM ovalbumin in demineralized water was set at pH 8.0 by the addition of 3 M NaOH using a pH-stat (Metrohm) at room temperature. Then, solid succinic anhydride was added in small aliquots during 30 min yielding a final concentration corresponding to either a mole ratio of 0.76 or 1.9 of succinic anhydride to lysine residues to produce two different degrees of succinylation. During the addition of succinic anhydride, the pH was kept at 8.0 (±0.1) by the addition of 1 M NaOH using pH-stat equipment. Next, the solution was stirred for another 2 h, followed by extensive dialysis against demineralized water at 4 °C and subsequent freeze-drying. The material (denoted in this work as OVA-26) was stored at −20 °C until use.

Chemical Characterization. The purity of ovalbumin, before and after modification, was checked using sodium dodecyl sulfate polyacrylamide gel electrophoresis (SDS-PAGE).[41] The apparent isoelectric point (IEP) of the ovalbumin variants was determined as described previously using isoelectric focusing.[42]

The degree of succinylation was determined by the method previously described[43] on the basis of the specific reaction between orthophthaldialdehyde (OPA) and free primary amino groups in proteins. In the presence of 2-(dimethyl amino) ethanethiol hydrochloride (DMA), these amino groups react to alkyl-iso-indole derivatives that show light absorption at 340 nm that can be monitored spectrophotometrically. All measurements were performed in triplicate.

The available number of carboxylic acid groups on the protein was determined by a spectrophotometric method using Woodward reagent K.[38] This method is based on the reaction between Woodward reagent K and free carboxylic acid groups resulting in an increase in absorbance at 269 nm. All measurements were performed in duplicate.

The number of free thiol groups was determined using the chromogenic Ellman's assay as has been published before,[44] in the presence and absence of 10% SDS using 2-nitro-5-mercaptobenzoic acid (DTNB).

Chemical Reactivity. The sulfhydryl-disulfhide exchange index (SEI) was determined according to a previously described protocol.[28] Three tenths milliliter of 2.2×10^{-4} M ovalbumin solutions was reacted with 2.7 mL 2.5×10^{-4} M 2-pyridine disulfide in a 10 mM sodium phosphate buffer (pH 7.0) at 25 °C and at 58 °C. The formation of 2-thiopyridine (2-TP) was spectrophotometrically followed at 343 nm as a function of time. The equation for this second-order reaction has been published.[45] The rate constant for pyridine disulfide reaction with protein (k) or GSH (k^*) is given in mole protein per second and was standardized by the rate constant for glutathione reaction with 2-pyridine disulfide determined under identical conditions and expressed as the sulfhydryl-disulfide exchange index (SEI). SEI is defined as $-\log(k/k^*)$.

Exposed Hydrophobicity. Fluorescence of *N*,*N*-dimethyl-6-propionyl-2-naphthylamine (PRODAN: BioChemika) was measured at 20 °C using a Varian Cary Eclipse Spectrofluorimeter. The amount of 0.19 mM PRODAN was dissolved in methanol. The final solution was filtered, and the concentration was determined at 365 nm using an extinction coefficient of $\epsilon_{365} = 1.45 \times 10^4$ M^{-1} cm^{-1}.[46] Fluorescence spectra were acquired at λ_{ex} 361 nm and λ_{em} 380−620 nm at a constant probe concentration of 9.2×10^{-7} M and at a varying protein concentration ranging from 7.1×10^{-6} to 1.4×10^{-4} M. One millilter

quartz cuvettes were used. The initial slope (S_0) was calculated from PRODAN fluorescence intensity per % protein as a function of the protein concentration. The reproducibility of S_0 was typically less than 5%.

Structural Characterization. Emission and excitation fluorescence spectra of 2.7 μM (charge-engineered) ovalbumin solutions in a phosphate buffer (10 mM, pH 7.0) were analyzed using a Perkin-Elmer (LS 50 B) luminescence spectrometer at 20 °C (±0.1 °C). The emission spectra from 300 to 400 nm were recorded at an excitation wavelength of 274 and 295 nm. Excitation and emission slit widths were 5 nm, and a scan speed of 120 nm/min was used. All spectra were corrected for the corresponding protein-free sample.

Far- and near-UV-circular dichroism (CD) experiments were performed as described previously[42] using a Jasco J-715 spectropolarimeter (Jasco Corp., Japan). Spectra were recorded as averages of 16 spectra. The scanning speed was 100 nm/min and the response time was 0.5 s with a bandwidth of 1.0 nm. The proteins were dissolved in 10 mM phosphate buffer at pH 7.0 at 2.3 μM for far-UV CD and 23.4 μM for near-UV CD. Cells with path lengths of 0.1 and 1 cm were used for far-UV CD and near-UV CD, respectively.

Thermal Unfolding. Differential scanning calorimetry (DSC) scans were obtained using a SETARAM (Caluire, France) micro DSC III with stainless steel 1 mL sample cells. Solutions were prepared with protein concentrations of 0.23 mM, pH 7.0 and also at 2.2 mM for OVA-26 at pH 7.0. A protein-free solution was used in the reference cell. The temperature was varied from 25 to 120 °C at a scan rate of 1 °C min^{-1}. Reference−reference baselines were obtained at the same scanning conditions and were subtracted from the sample curves. The measurements were performed in duplicate.

Equilibrium Unfolding. Urea titration experiments were performed to monitor the change in fluorescence intensity upon the addition of urea. A 10 mM phosphate buffer solution at pH 7.0 was prepared using reagent grade salts NaH_2PO_4 and Na_2HPO_4 (Merck) in demineralized water. An 8 M urea stock solution was prepared by dissolving 0.755 g of urea (Merck) per mL in a 10 mM phosphate buffer solution. The protein stock solutions were prepared by diluting the protein with 10 mM phosphate buffer pH 7.0 at 23.9 μM. One hundred microliters of the protein stock solution was then diluted with 2 mL of urea solution with final concentrations ranging from 0 to 6 M. Prior to the measurement, the samples were incubated for 24 h at room temperature which is required to reach stable fluorescence intensity (unpublished results). After incubation, the sample was placed into a thermostatted 1 mL quartz cell at 25 °C. The fluorescence emission was recorded between 300 and 450 nm upon excitation at 295 nm on a Varian Cary Eclipse Spectrofluorimeter. The slit widths were set at 5 nm.

Aggregation Kinetics. For the determination of the heat-induced aggregation kinetics, different series of screw-cap vials containing 5 mL of 10 mg/mL protein solution (pH 7.0) were heated for various times up to 24 h at 72.0, 66.8, 72.0, and 69.4 °C (corresponding to the temperatures where the rate constant for the generation of denatured particles is expected to be similar, on the basis of the activation energy and corresponding denaturation temperature as found by DSC for the individual protein variants, as described in the Results section). Previously, it was already shown for native ovalbumin that the denaturation temperature was not significantly affected by the protein concentration in the range from 0.5 to 10 mg/mL.[22] Next, the vials were cooled in ice water, and the protein solutions were diluted to a final concentration of monomeric protein between 0.1 and 5 mg/mL, to be within the calibration range for size exclusion chromatographic analysis. After centrifugation at 20 000*g* for 5 min at room temperature, the exact concentration of monomeric protein in the supernatant was determined by HPSEC (Phenomenex BioSep-SEC-S2000 column, 300 × 7.5 mm) using UV detection at 280 nm. The intensity (taken as the integral in the monomeric fraction elution profile) was calibrated by a series of centrifuged protein solutions with known concentration applied to the same column.

Acknowledgment. The authors thank Prof. Sanchez-Ruiz, Dr. Ton Marcelis, and Prof. Willem Norde for stimulating discussions, Prof. Voragen for careful reading of the manuscript, and Ir. Hans Kosters for carrying out the chromogenic Ellman's assay.

Supporting Information Available. (1) Near-UV CD spectra of the charge variants of ovalbumin demonstrating a comparable tertiary fold and (2) far-UV CD spectra of more extreme modified variants illustrating the loss of native structure when higher degrees of modification are employed. This material is available free of charge via the Internet at http://pubs.acs.org.

References and Notes

(1) Narang, H. K. J. *Neuropathol. Exp. Neurol.* **1980**, *39*, 621−631.
(2) Merz, P. A.; Wisniewski, H. M.; Somerville, R. A.; Bobin, S. A.; Masters, C. L.; Iqbal, K. *Acta Neuropathol. (Berlin)* **1983**, *60*, 113−124.
(3) Kelly, J. W. *Curr. Opin. Struct. Biol.* **1998**, *8*, 101−106.
(4) Lansbury, P. T. *Proc. Natl. Acad. Sci. U.S.A.* **1999**, *96*, 3342−3344.
(5) Lopez de la Paz, M. L.; Serrano, L. *Proc. Natl. Acad. Sci. U.S.A.* **2004**, *101*, 87−92.
(6) Malisauskas, M.; Zamotin, V.; Jass, J.; Noppe, W.; Dobson, C. M.; Morozova-Roche, L. A. *J. Mol. Biol.* **2003**, *330*, 879−890.
(7) Uversky, V. N.; Fink, A. L. *Biochim. Biophys. Acta* **2004**, *1698*, 131−153.
(8) Hwang, W.; Zhang, S.; Kamm, R. D.; Karplus, M. *Proc. Natl. Acad. Sci. U.S.A.* **2004**, *101*, 12916−12921.
(9) Guijarro, J. I.; Sunde, M.; Jones, J. A.; Campbell, I. D.; Dobson, C. M. *Proc. Natl. Acad. Sci. U.S.A.* **1998**, *95*, 4224−4228.
(10) Frankenberg, N.; Welker, C.; Jaenicke, R. *FEBS Lett.* **1999**, *454*, 299−302.
(11) Villegas, V.; Zurdo, J.; Filimonov, V. V.; Aviles, F. X.; Dobson, C. M.; Serrano, L. *Protein Sci.* **2000**, *9*, 1700−1708.
(12) Zurdo, J.; Guijarro, J. I.; Jiménez, J. L.; Saibil, H. R.; Dobson, C. M. *J. Mol. Biol.* **2001**, *311*, 325−340.
(13) Lopez De La Paz, M.; Goldie, K.; Zurdo, J.; Lacroix, E.; Dobson, C. M.; Hoenger, A.; Serrano, L. *Proc. Natl. Acad. Sci. U.S.A.* **2002**, *99*, 16052−16057.
(14) Chiti, F.; Calamai, M.; Taddei, N.; Stefani, M.; Ramponi, G.; Dobson, C. M. *Proc. Natl. Acad. Sci. U.S.A.* **2002**, *99*, 16419−16426.
(15) Chiti, F.; Stefani, M.; Taddei, N.; Ramponi, G.; Dobson, C. M. *Nature* **2003**, *424*, 805−808.
(16) Nakamura, R.; Sugiyama, H.; Sato, Y. *Agric. Biol. Chem.* **1978**, *42*, 819−824.
(17) Pots, A. M.; ten Grotenhuis, E.; Gruppen, H.; Voragen, A. G. J.; de Kruif, K. G. *J. Agric. Food Chem.* **1999**, *47*, 4600−4605.
(18) Bogin, O.; Levin, I.; Hacham, Y.; Tel-Or, S.; Peretz, M.; Frolow, F.; Burstein, Y. *Protein Sci.* **2002**, *11*, 2561−2574.
(19) Loladze, V. V.; Ibarra-Molero, B.; Sanchez-Ruiz, J. M.; Makhatadze, G. I. *Biochemistry* **1999**, *38*, 16419−16423.
(20) Gounaris, A. D.; Perlmann, G. E. *J. Biol. Chem.* **1967**, *242*, 2739−2745.
(21) Nakagawa, Y.; Capetillo, S.; Jirgensons, B. *J. Biol. Chem.* **1972**, *247*, 5703−5708.
(22) Kosters, H.; Broersen, K.; de Groot, J.; Simons, J. W. F. A.; Wierenga, P.; de Jongh, H. H. J. *Biotechnol. Bioeng.* **2003**, *84*, 61−70.
(23) Koseki, T.; Kitabatake, N.; Doi, E. *Food Hydrocolloids* **1989**, *3*, 123−134.
(24) Veerman, C.; de Schiffart, G.; Sagis, L. M. C.; van der Linden, E. *Int. J. Biol. Macromol.* **2003**, *33*, 121−127.
(25) Weijers, M. E.; Barneveld, P. A.; Cohen Stuart, M. A.; Visschers, R. W. *Protein Sci.* **2003**, *12*, 2693−2703.
(26) Wierenga, P. A.; Meinders, M. B. J.; Egmond, M. R.; Voragen, A. G. J.; de Jongh, H. H. J. *J. Phys. Chem. B* **2005**, *109*, 16946−16952.
(27) Alizadeh-Pasdar, N.; Li-Chan, E. C. Y. *J. Agric. Food Chem.* **2000**, *48*, 328−334.
(28) Owusu-Apenten, R. K.; Chee, C.; Hwee, O. P. *Food Chem.* **2003**, *83*, 541−545.
(29) Sanchez-Ruiz, J. M.; Lopez-Lacomba, J. L.; Cortijo, M.; Mateo, P. L. *Biochemistry* **1988**, *27*, 1648−1652.
(30) Sali, D.; Bycroft, M.; Fersht, A. R. *J. Mol. Biol.* **1991**, *220*, 779−788.
(31) Ma, C.-Y.; Holme, J. *J. Food Sci.* **1982**, *47*, 1454−1459.
(32) Gossett, P. W.; Baker, R. C. *J. Food Sci.* **1983**, *48*, 1391−1394.

(33) Xiao, L.; Honig, B. *J. Mol. Biol.* **1999**, *289*, 1435−1444.
(34) Godoy-Ruiz, R.; Perez-Jimenez, R.; Ibarra-Molero, B.; Sanchez-Ruiz, J. M. *J. Mol. Biol.* **2004**, *336*, 313−318.
(35) Cavagnero, S.; Debe, D. A.; Zhou, Z. H.; Adams, M. W. W.; Chan, S. I. *Biochemistry* **1998**, *37*, 3369−3376.
(36) Kuznetsova, I. M.; Turoverov, K. K.; Uversky, V. N. J. *Proteome Res.* **2004**, *3*, 485−494.
(37) Weijers, M. E.; Broersen, K.; Barneveld, P. A.; Cohen Stuart, M. A.; Hamer, R. J.; de Jongh, H. H. J.; Visschers, R. W. *Protein Sci.*, submitted for publication, 2007.
(38) Kosters, H.; de Jongh, H. H. J. *Anal. Chem.* **2003**, *75*, 2512−2516.
(39) Hoare, D. G.; Koshland, D. E. *J. Biol. Chem.* **1967**, *242*, 2447−2453.
(40) Klotz, I. M. *Methods Enzymol.* **1967**, *11*, 567−580.
(41) Laemmli, U. K. *Nature* **1970**, *227*, 680−685.
(42) Broersen, K.; Voragen, A. G. J.; Hamer, R. J.; de Jongh, H. H. J. *Biotechnol. Bioeng.* **2004**, *86*, 78−87.
(43) Church, F. C.; Swaisgood, H. E.; Porter, D. H.; Catignani, G. L. *J. Dairy Sci.* **1983**, *66*, 1219−1227.
(44) Ellman, G. L. *Arch. Biochem. Biophys.* **1959**, *82*, 70−77.
(45) Owusu-Apenten, R. K.; Galani, D. *J. Sci. Food. Agric.* **2000**, *80*, 447−452.
(46) Weber, G.; Farris, F. J. *Biochemistry* **1979**, *18*, 3075−3078.
(47) van Teeffelen, A. M. M.; Broersen, K.; de Jongh, H. H. J. *Protein Sci.* **2005**, *14*, 2187−2194.

BM0612283